

UC Davis

UC Davis Previously Published Works

Title

Genomic prediction of strawberry resistance to postharvest fruit decay caused by the fungal pathogen *Botrytis cinerea*

Permalink

<https://escholarship.org/uc/item/23x4j138>

Journal

G3: Genes, Genomes, Genetics, 12(1)

ISSN

2160-1836

Authors

Petrasch, Stefan
Mesquida-Pesci, Saskia D
Pincot, Dominique DA
[et al.](#)

Publication Date






2022-01-04

DOI

10.1093/g3journal/jkab378

Peer reviewed

Genomic prediction of strawberry resistance to postharvest fruit decay caused by the fungal pathogen *Botrytis cinerea*

Stefan Petrasch, Saskia D. Mesquida-Pesci, Dominique D. A. Pincot , Mitchell J. Feldmann , Cindy M. López, Randi Famula , Michael A. Hardigan, Glenn S. Cole, Steven J. Knapp *, and Barbara Blanco-Ulate *

Department of Plant Sciences, University of California, Davis, Davis, CA 95616, USA

*Corresponding author: Department of Plant Sciences, University of California, Davis, One Shields Avenue, Davis, CA 95616, USA.
Email: sjknapp@ucdavis.edu (S.J.K.); bblanco@ucdavis.edu (B.B.U.)

Abstract

Gray mold, a disease of strawberry (*Fragaria × ananassa*) caused by the ubiquitous necrotroph *Botrytis cinerea*, renders fruit unmarketable and causes economic losses in the postharvest supply chain. To explore the feasibility of selecting for increased resistance to gray mold, we undertook genetic and genomic prediction studies in strawberry populations segregating for fruit quality and shelf life traits hypothesized to pleiotropically affect susceptibility. As predicted, resistance to gray mold was heritable but quantitative and genetically complex. While every individual was susceptible, the speed of symptom progression and severity differed. Narrow-sense heritability ranged from 0.38 to 0.71 for lesion diameter (LD) and 0.39 to 0.44 for speed of emergence of external mycelium (EM). Even though significant additive genetic variation was observed for LD and EM, the phenotypic ranges were comparatively narrow and genome-wide analyses did not identify any large-effect loci. Genomic selection (GS) accuracy ranged from 0.28 to 0.59 for LD and 0.37 to 0.47 for EM. Additive genetic correlations between fruit quality and gray mold resistance traits were consistent with prevailing hypotheses: LD decreased as titratable acidity increased, whereas EM increased as soluble solid content decreased and firmness increased. We concluded that phenotypic and GS could be effective for reducing LD and increasing EM, especially in long shelf life populations, but that a significant fraction of the genetic variation for resistance to gray mold was caused by the pleiotropic effects of fruit quality traits that differ among market and shelf life classes.

Keywords: *Fragaria × ananassa*; *Botrytis cinerea*; breeding; necrotroph; genome-wide association study; disease resistance; whole-genome regression

Introduction

The fleshy fruits produced by strawberry (*Fragaria × ananassa*), tomato (*Solanum lycopersicum*), and many other horticulturally important plants are susceptible to postharvest decay by gray mold, a devastating disease caused by the necrotrophic fungal pathogen *Botrytis cinerea* (Jarvis 1962; van Baarlen et al. 2007; Williamson et al. 2007; Dean et al. 2012; Elad et al. 2016; Petrasch et al. 2019a). *Botrytis cinerea* can infect most organs of the plant but is especially destructive on ripe fruit and senescent tissues of dicotyledonous hosts (Jarvis 1962; Dewey and Grant-Downton 2016). Gray mold renders strawberries unmarketable and often causes significant postharvest losses under conditions favorable for pathogen growth (Barritt 1980; Ries 1995; Dean et al. 2012; Petrasch et al. 2019a). The mechanisms of defense against *B. cinerea* are physiologically and genetically complex and markedly differ from the gene-for-gene resistance and programmed cell death mechanisms commonly triggered by biotrophic pathogens (Elad and Evensen 1995; Glazebrook 2005; Lorang 2019; Caseys et al. 2021). As with other necrotrophic pathogens, *B. cinerea* pathogenesis is promoted by fruit ripening and host cell death (Elad and Evensen 1995; Elad et al. 2016; Lorang 2019).

Consequently, genetic variation for resistance to gray mold tends to be subtle, limited, and quantitative, which undoubtedly underlies the paucity of studies on breeding for resistance to this pathogen (Finkers et al. 2007a; Williamson et al. 2007; Rowe and Kliebenstein 2008; Lorang 2019; Zhang et al. 2019; Caseys et al. 2021).

Because natural genetic resistance has been insufficient to prevent postharvest gray mold disease development, preharvest fungicides are often applied to suppress pathogen growth and minimize postharvest losses (Legard et al. 1997, 2005; Leroux 2007; Elad et al. 2016; Cosseboom et al. 2019). Controlling *B. cinerea* with fungicides is difficult because the airborne inoculum is present year round, the host–pathogen interactions are complicated, and the pathogen rapidly evolves resistance to fungicides, particularly after repeated applications of specific chemicals (Jarvis 1962; Leroux 2007; Williamson et al. 2007; Cosseboom et al. 2019; Zhang et al. 2019; Caseys et al. 2021). Moreover, preharvest foliar applications of fungicides have not been shown to be effective for reducing postharvest gray mold incidence in strawberry fruit possibly because many fruit infections arise from contaminated

Received: June 07, 2021. Accepted: October 08, 2021

© The Author(s) 2021. Published by Oxford University Press on behalf of Genetics Society of America.

This is an Open Access article distributed under the terms of the Creative Commons Attribution License (<https://creativecommons.org/licenses/by/4.0/>), which permits unrestricted reuse, distribution, and reproduction in any medium, provided the original work is properly cited.

flower tissues (van Kan 2006; van Baarlen et al. 2007; Williamson et al. 2007; Veloso and van Kan 2018; Petrasch et al. 2019a).

The development of gray mold resistant cultivars has been challenging in strawberry and other hosts because most genotypes are highly susceptible, strong sources of natural genetic resistance have not been identified, and resistance mechanisms are quantitative (Barritt 1980; van Kan 2006; Finkers et al. 2007a, 2007b, 2008; Williamson et al. 2007; Seijo et al. 2008; Lewers et al. 2012; Petrasch et al. 2019a; Zhang et al. 2019; Caseys et al. 2021). The feasibility of selecting for increased resistance to gray mold has not been deeply explored in strawberry, a species where limited studies have been undertaken to shed light on the genetics of resistance and assess genetic variation for resistance (Barritt 1980; Seijo et al. 2008; Lewers et al. 2012). The problem of breeding for resistance to gray mold has been most extensively studied in tomato, albeit without achieving robust or foolproof solutions (Finkers et al. 2007a, 2007b, 2008). Genetic studies in tomato and *Arabidopsis* leaves have identified multiple small-effect quantitative trait loci (QTL) that only account for a small fraction of the genetic variation for resistance, seldom translate across genetic backgrounds, and have not solved the problem of breeding for resistance to gray mold (Finkers et al. 2007a, 2007b, 2008; Rowe and Kliebenstein 2008). Although genetic studies of similar depth and breadth have not been undertaken in strawberry, previous studies have not uncovered strong sources of resistance to gray mold (Barritt 1980; Bestfleisch et al. 2015; Seijo et al. 2008; Lewers et al. 2012).

We suspected that selection for increased fruit firmness and other fruit quality traits that extend shelf life pleiotropically increased resistance (decreased susceptibility) to gray mold in strawberry. While hypotheses can be formulated from insights gained from genetic studies in tomato and other hosts (Blanco-Ulate et al. 2016a, 2016b; Petrasch et al. 2019b; Zhang et al. 2019; Caseys et al. 2021), natural genetic resistance appears to be negligible and quantitative and additive genetic correlations between gray mold resistance and fruit quality phenotypes are unknown in strawberry (Jarvis 1962; Rhainds et al. 2002; Chandler et al. 2006; Seijo et al. 2008; González et al. 2009; Lewers et al. 2012; González et al. 2013; Bestfleisch et al. 2015; Petrasch et al. 2019a). The susceptibility of strawberry fruit to *B. cinerea* increases during ripening (Jarvis 1962), which suggests that susceptibility factors accumulate independent of defense mechanisms during fruit maturation and senescence, as is typical for this necrotroph (Williamson et al. 2007; Zhang et al. 2019; Caseys et al. 2021; Silva et al. 2021). Changes in fruit firmness and other fruit quality traits associated with fruit maturation and ripening in tomato have been shown to increase susceptibility to *B. cinerea* (Blanco-Ulate et al. 2016a, 2016b; Silva et al. 2021). Although previous studies have been somewhat inconclusive in strawberry, firm-fruited cultivars are predicted to be more resistant to *B. cinerea* than soft-fruited cultivars (Gooding 1976; Barritt 1980). Moreover, ripening-induced differences in proanthocyanidin and anthocyanin accumulation have been predicted to affect *B. cinerea* resistance in tomato and strawberry (Jersch et al. 1989; Zhang et al. 2013; Bassolino et al. 2013).

To more deeply explore the genetics of resistance to gray mold and assess the feasibility of applying genomic selection (GS) for increased resistance to gray mold in strawberry, we developed and studied training populations segregating for fruit quality traits predicted to affect shelf life. Genomic prediction approaches are particularly attractive for postharvest traits that are difficult and costly to phenotype in strawberry but still require sufficient accuracy to complement phenotypic selection

and achieve genetic gains (Heffner et al. 2010; Jannink et al. 2010; Lin et al. 2014; VanRaden 2020). The training populations for our studies were developed from crosses between firm-fruited long shelf life (LSL) cultivars and soft-fruited short shelf life (SSL) cultivars. Although the gray mold resistance phenotypes of the parents of these populations were unknown, our hypothesis was that selection for extended shelf life has pleiotropically increased resistance to gray mold in strawberry, primarily because fruit of LSL cultivars deteriorate more slowly in postharvest storage than those of SSL cultivars. We describe a highly repeatable artificial inoculation protocol for gray mold resistance phenotyping developed for the GS studies described herein. Finally, we discuss the prospects for increasing genetic gains for resistance to gray mold through the application of genomic prediction approaches.

Materials and methods

Plant materials and study design: shelf life assessment of modern LSL cultivars

Shelf life studies were conducted with fruit harvested from five day-neutral cultivars (“UCD Royal Royce,” “UCD Valiant,” “UCD Moxie,” “Cabrillo,” and “Monterey”) and three “summer-plant” (“UCD Finn,” “UCD Mojo,” and “Portola”) cultivars (the “UCD” prefixes are hereafter dropped from the cultivar names) grown on organic and conventional farms using the standard production practices of commercial growers in coastal California. The day-neutral cultivars were grown in 20-plant plots on three commercial farms, one organic and two conventional, in Santa Maria and Prunedale, California in 2017–2018 with harvests for postharvest studies on June 22 and 27, July 30, and August 1, 2018, July 30, 2018. The summer-plant cultivars were grown in 20-plant plots on three commercial farms, one organic and two conventional, in Oxnard and Santa Maria, CA in 2018–2019 with harvests for postharvest studies on September 27 and 30, November 1 and 18, and December 4, 2019.

To assess shelf life and estimate gray mold incidence, fruit was harvested on two dates at each location and stored in a dark walk-in cooler maintained at approximately 4°C and 90–95% relative humidity for 21 days postharvest (dph). Harvest dates were June 22 and 27, July 30, and August 1, 2018, for day-neutral cultivars and September 27 and 30, November 1, 18, and 21, and December 4, 2019, for summer-plant cultivars. Two 0.45 kg samples of fruit were collected at each harvest and placed in 18.4 cm × 12.1 cm × 6.2 cm vented plastic clamshells, one of which was stored undisturbed for visual phenotyping and another of which was used for destructive fruit quality trait measurements at three time points for summer-plant experiment (0, 7, and 14 dph) and four time points for the day-neutral experiment (0, 7, 14, and 21 dph). Soluble solid content (SSC; °Brix), fruit firmness (g-force), fruit weight (g/fruit), fungal decay incidence (% of clamshell), and marketability were recorded at each time point. The latter was visually scored on a 1–5 scale, where 1 = very good, 2 = good, 3 = fair, 4 = poor, and 5 = very poor (Mitcham et al. 1996; do Nascimento Nunes 2015). Four fruit were randomly selected from each clamshell at each time point for fruit firmness and SSC measurements. Firmness was measured using a handheld penetrometer (QA Supplies Model FT02) with a 3 mm probe. SSC (°Brix) was measured in the juice of macerated fruit with a digital handheld refractometer (Atago Model PAL-1). Statistical analyses of these experiments were separately performed using the R package *lme4* (Bates et al. 2015) with cultivar as a fixed effect and with location and cultivar × location interaction as random effects. Estimated marginal means (EMMs) and

linear contrasts between cultivar EMMs were estimated using the R package *emmeans* (Lenth 2021).

Plant materials and study design: genetics of gray mold resistance

Seeds of five *F. × ananassa* full-sib families were harvested from crosses produced in a greenhouse at UC Davis in the winter of 2018: Royal Royce × Primella (PI551422), Royal Royce × Madame Moutot (PI551632), Royal Royce × Tangi (PI551481), Royal Royce × Earlimiss (PI551862), and 05C197P002 × 16C108P065. These families constituted the multifamily training population developed for genomic prediction and other analyses. Seeds were scarified and germinated the week of June 18–22, 2018. Seedlings were established and grown in a greenhouse until they were transplanted to the field on October 5, 2018, at the UC Davis Wolfskill Experiment Orchard (WEO), Winters, CA, USA. The field site was prepared with a disk-harrow and ring-roller and smoothed with a spring-tooth harrow. The soil was fumigated on May 14, 2018, with Pic-Clor 60[®] (1, 3-dichloropropene 39% and chloropicrin 59.6%; Cardinal Professional Products, Woodland, CA, USA) at a rate of 474.7 kg/ha. Subsequent to fumigation, planting beds were mechanically shaped to a height of 30.5 cm, width of 50.8 cm, base of 121.9 cm with center-to-center spacing of 152.4 cm between beds, and a furrow width of 30.5 cm. Seedlings were transplanted to planting beds on October 15, 2018, in a single-centered row with 55.9 cm between plants within the row. The number of individuals that produced sufficient fruit for the postharvest study of resistance to gray mold were $n=86$ for Royal Royce × Primella, $n=82$ for Royal Royce × Madame Moutot, $n=78$ for Royal Royce × Tangi, $n=92$ for Royal Royce × Earlimiss, and $n=42$ for 05C197P002 × 16C108P065. The parents were planted from bare-root plants produced in a commercial high-elevation nursery in Dorris, CA, USA. The population was grown through June 30, 2019, irrigated as needed to prevent water stress, and hand weeded throughout the growing season. Fruit were harvested on from May 15 to June 7, 2019. Additional Royal Royce × Tangi full-sib individuals ($n=155$) were grown, handled, and phenotyped in 2019–2020 exactly as described above for the 2018–2019 experiment (phenotypic data were collected for 233 Royal Royce × Tangi individuals over two years). Fruit were harvested May 8–29, 2020.

DNA isolation and single-nucleotide polymorphism marker genotyping

DNA was extracted from 0.2 g of dried young leaf tissue with the E-Z 96 Plant DNA Kit (Omega Bio-Tek, Norcross, GA, USA) per the manufacturer's instructions, though the protocol was modified by adding Proteinase K to the lysis buffer to a final concentration of 0.2 mg/ml and extending lysis incubation to 45 min. at 65°C to increase the quality and yield of the DNA. Single-nucleotide polymorphisms (SNPs) were genotyped using the 50K Axiom SNP array (Hardigan et al. 2020), and SNP calls were generated using the Affymetrix Axiom Suite (v1.1.1.66). The raw genotypic data were filtered to identify polymorphic SNP markers with clear and well separated homozygous and heterozygous genotypic classes and eliminate individual SNP markers with minor allele frequencies < 0.05 and any missing data. This process yielded 11,946 SNPs for the training population ($n=380$) studied in 2019 and 9962 SNPs for the Royal Royce × Tangi full-sib population ($n=233$) studied in 2019 and 2020.

Gray mold resistance phenotyping

We developed a high-throughput protocol for postharvest phenotyping of *B. cinerea* disease progression and symptom development on ripe fruit. Spore suspensions of the *B. cinerea* strain B05.10 (Büttner et al. 1994; Quidde et al. 1998) were produced from spores grown on potato dextrose agar as described by Petrasch et al. (2019b). Uniformly ripe fruit were harvested at sunrise, avoiding fruit that were under- or over-ripe. The fruit were immediately transferred to cold storage (2.5°C) and inoculated the day of harvest. Several incubation temperatures (2.5°C, 5.0°C, 10.0°C, and 20.0°C) were tested to identify the optimum temperature for *B. cinerea* growth and development with a minimum of contamination from other postharvest decay pathogens. Fruit were placed on 30-cell plastic egg hatching trays with dimensions of 29 cm × 29 cm and 4.5 cm × 4.5 cm cells. The fruit were punctured once near the center with a 3 mm sterile pipette tip to an approximate depth of 1–2 mm. Ten μl of the *B. cinerea* conidia suspension (500 conidia/ μl) was placed on the surface of the puncture. The inoculated fruit were incubated in a growth chamber at 10°C and 95% humidity for 14 days. Disease symptoms were assessed daily after inoculation by manually measuring lesion diameter (LD) and determining the number of days until external mycelium (EM; white or gray hyphae) was evident on the surface of the fruit near the wound site. Fruit were phenotyped until mycelia covered the entire surface of the fruit. Spoiled fruit with infections outside of the inoculation site or caused by decay organisms other than *B. cinerea* were removed from the experiment. Genome-wide association study (GWAS), QTL mapping, and GS analyses were applied to LD at 8 days postinoculation (dpi) and EM.

Fruit quality phenotyping

Fruit quality phenotypes were measured on one to four fruit harvested from individuals in the multifamily population at harvest. The fruit were photographed with a Sony α 6000 camera equipped with an E PZ 16–50 mm F3.5–5.6 OSS lens (SONY, Tokyo, Japan). Photographs were processed with a custom macro in Fiji (Schindelin et al. 2012; Rueden et al. 2017) to obtain RGB color metrics (Supplementary File S1). RGB colors were subsequently converted into Lab colors using the `convertColor()` function in R (R Core Team 2021). Fruit firmness (maximum resistance g-force) and fruit diameter (mm) were assessed on whole fruit using a TA.XT plus Texture Analyzer with a TA-53 3 mm puncture probe (Stable Micro Systems Ltd., Goldaming, United Kingdom). Fruit samples were frozen at -20°C in Whirl-Pak[®] Homogenizer Blender Filter Bags (Nasco, Fort Atkinson, WI, USA) for quantifying titrable acidity (TA; %), SSC ($^{\circ}\text{BRIX}$), and total anthocyanin concentration (AC; $\mu\text{g/ml}$). TA percentages were quantified with a Metrohm Robotic Titrosampler System from 1 to 5 ml of the defrosted homogenized fruit juice (Metrohm AG, Herisau, Switzerland). SSC was measured from approximately 200 μl of juice on an RX-5000 α -Bev Refractometer (ATAGO Co. Ltd., Tokyo, Japan). Total AC was measured from a 25 μl sample of juice in 200 μl 1% HCl in methanol by reading absorption at a wavelength of 520 nm on a Synergy HTX platereader equipped with Gen5 software (Molecular Devices, San Jose, California, USA). A standard curve ($y = sx + i$) was calculated for quantifying AC using a dilution series of pelargonidin (Sigma Aldrich, St. Louis, MI, USA) from 0 to 300 $\mu\text{g/ml}$ in 50 $\mu\text{g/ml}$ increments, where y was absorption readings for the pelargonin dilution series, s was the slope, x was the concentration of pelargonin in

the dilution series, and i was the intercept. AC was estimated by $(A - i)/s$, where A was the absorption reading.

Statistical analyses: genetic and QTL mapping and GWAS

GWAS approaches were applied to search for marker-trait associations in the multifamily training population and the Royal Royce \times Tangi population. EMMs for LD and EM were estimated from subsamples and biological replications using the R package *emmeans* (Lenth 2021). GWAS analyses were applied using the *GWAS()* function in the R package *rrBLUP* with SNP genotypes (AA , Aa , and aa) coded -1 , 0 , and 1 , respectively (Endelman 2011). The genomic relationship matrix was used to correct for population stratification (Endelman 2011). The genomic inflation factor (λ) was 0.60 for LD and 0.71 for EM for analyses of the multifamily population and 1.09 for LD and 1.00 for EM for analyses of the Royal Royce \times Tangi population. The Bonferroni-corrected threshold for statistical significance was $-\log_{10}(0.05/k)$ where k is the number of SNPs used in the analysis. The Bonferroni-corrected threshold was $-\log_{10}(4.2 \times 10^6)$ for the multifamily population and $-\log_{10}(5.0 \times 10^6)$ for the Royal Royce \times Tangi population.

Parent-specific genetic maps were developed for each full-sib family using a custom PERL script pipeline utilizing the R packages *BatchMap* and *onemap* (Schiffthaler et al. 2017; Margarido et al. 2007; Supplementary File S4). This pipeline was used to bin cosegregating markers, calculate pairwise recombination fractions, assign markers to linkage groups, and estimate linkage disequilibrium (LD) statistics between groups of markers. Specifically, initial linkage groups (representing chromosomal fragments or sub-linkage groups) were assembled using a LOD threshold of 10.0 and a maximum recombination fraction of 0.08 . These thresholds typically generate more linkage groups than chromosomes. These chromosomal fragments or sub-linkage groups were then merged manually based on inter-group linkage disequilibrium statistics and %-identity against the physical genome (Edger et al. 2019). The RECORD algorithm (Van Os et al. 2005) was used to estimate marker order and genetic distances across a sliding window of 25 markers with a window overlap of 18 markers.

QTL analyses were applied to parent-specific genetic maps within each full-sib family using the *scanone()* function and Haley-Knott regression (Haley and Knott 1992) as implemented in the R package *qtl* (Broman et al. 2003). The null hypothesis of no significant difference between SNP marker genotypes was tested for each locus using backcross equivalent contrasts; specifically, $\bar{y}_{Aa} - \bar{y}_{aa}$ for SNP markers segregating in the female parent and $\bar{y}_{aa} - \bar{y}_{Aa}$ for SNP markers segregating in the male parent, where Aa is a heterozygote and aa is a homozygote. The null hypothesis of no QTL effect was rejected when the likelihood odds (LOD) ratio for the SNP marker effect exceeded the genome-wide LOD significance threshold empirically estimated by permutation with 1000 randomly drawn samples (Churchill and Doerge 1994).

We searched the *F. × ananassa* “Camarosa” reference genome (Edger et al. 2019) for QTL-associated candidate genes with putative biotic stress or disease resistance gene function annotations. Gene Ontology annotations were filtered to identify candidate genes predicted to be involved in plant-pathogen interactions. Candidate genes were annotated using the KEGG Automated Annotation Server (KAAS; Moriya et al. 2007) pipeline and filtered pathways. The iTAK pipeline was used to predict the presence of transcription factors and protein kinases (Zheng et al. 2016).

Statistical analyses: estimation of genetic and genomic prediction parameters

The repeatability on a progeny mean-basis (R) was estimated for each trait from multiple subsamples/individual (fruit/individual) by $R = \sigma_B^2 / (\sigma_B^2 + \sigma_W^2 / \bar{s})$, where σ_B^2 is the between-individual variance component, σ_W^2 is the among subsamples nested in individuals variance component, \bar{s} is the harmonic mean number of subsamples/individual, and \bar{s} was 2.4 in the multifamily population and 3.6 in the Royal Royce \times Tangi population. Variance components were estimated using REML in the R package *lme4* (Bates et al. 2015). Narrow-sense genomic heritability (h^2) was estimated for each trait from the mean of 1000 REML estimates of the additive genetic and phenotypic variance components from 1000 Markov Chain Monte Carlo (MCMC) samples drawn for cross-validation using G-BLUP (Endelman 2011).

Genomic estimated breeding values (GEBVs) were estimated for each trait by applying three whole-genome regression methods in both training populations—genomic best linear unbiased prediction (G-BLUP), reproducing kernel Hilbert spaces (RKHS), and support vector machine (SVM). G-BLUP, RKHS, and SVM mixed model analyses were performed using the *kinBLUP()* function of *rrBLUP* (Endelman 2011), the *BGLR()* function of the R package *BGLR* (Pérez and de Los Campos 2014), and the *svm()* function of R package *e1071* (Meyer et al. 2019), respectively. The kernel for RKHS was determined using the multikernel averaging method (de Los Campos et al. 2010). Cross-validation analyses were performed for each population \times trait \times whole-genome regression (WGR) method using 1000 MCMC samples/analysis, where GEBVs were estimated from a random sample of 80% of the individuals and predicted for the GEBVs for the other 20% of the individuals in each sample; 100% of the subsamples/individual were used for these analyses. We replicated these cross-validation analyses using a single randomly selected subsample/individual, where GEBVs were estimated from a random sample of 80% of the individuals (with a single subsample/individual) and predicted the GEBVs for the other 20% of the individuals. GS accuracy was estimated for each of the nine analyses as the correlation between the phenotypic means (EMMs) and GEBVs ($r_{\bar{y}, \text{GEBV}}$) for each trait from 1000 MCMC samples/analysis.

Results and discussion

Natural postharvest gray mold infections on fruit of LSL cultivars

Our studies were partly motivated by the observation that gray mold infections were uncommon between 0 and 14 dpi in a series of postharvest shelf life studies of modern LSL strawberry cultivars (Figure 1; Supplementary Figure S1). The fruit for these studies were harvested from five day-neutral cultivars (“Royal Royce,” “Valiant” “Moxie” “Cabrillo,” and “Monterey”) and three summer-plant cultivars (“Finn,” “Mojo” and “Portola”) grown on commercial farms in coastal California (Figure 1; Supplementary Figure S1). These studies produced several insights. Gray mold infections were rarely observed before 14 – 16 dph on any of the cultivars tested (Figure 1; Supplementary Figure S1). Statistically significant differences in gray mold incidence were not observed among day-neutral cultivars ($P = 0.87$) or summer-plant cultivars ($P = 0.98$) or between organically and conventionally produced fruit ($P = 0.27$ for day-neutral and $P = 0.68$ for summer-plant cultivars). Cultivar \times location interactions were nonexistent—REML estimates of the cultivar \times environment interaction variance component were zero in both studies ($P = 1$).

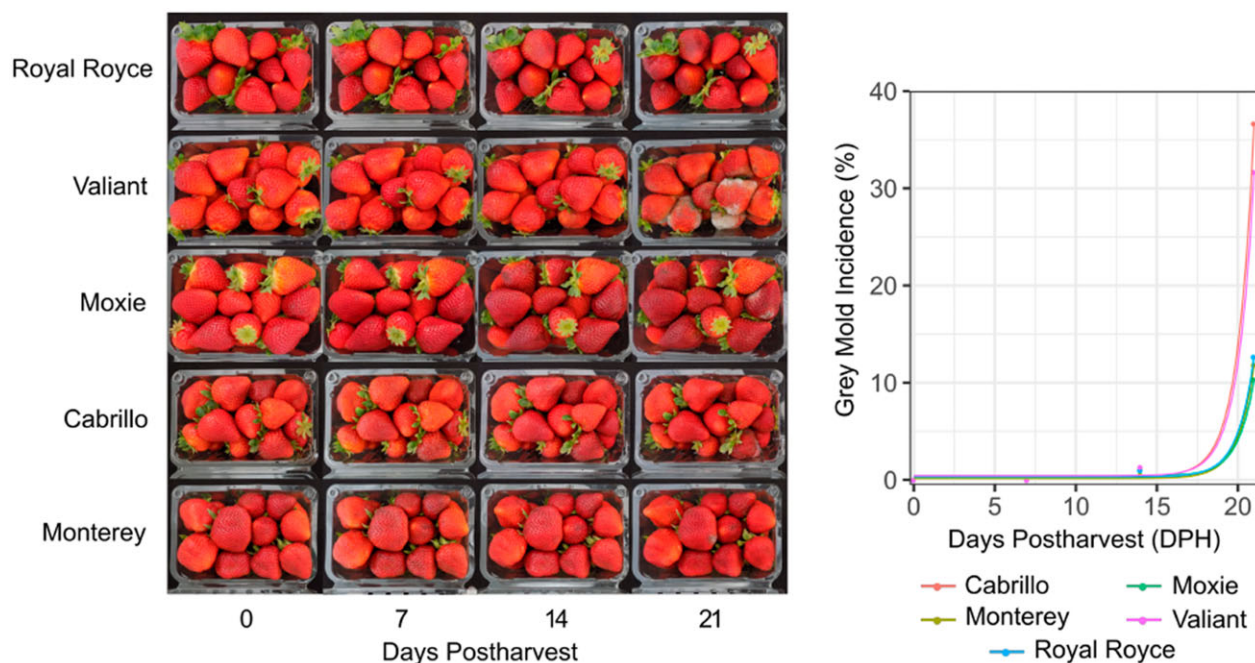


Figure 1 Postharvest visual appearance of cold stored fruit of LSL day-neutral cultivars grown in coastal California. Fruit of “Royal Royce,” “Valiant,” “Moxie,” “Cabrillo,” and “Monterey” were harvested June 22 and 27, July 30, and August 1, 2018 from commercial farms in Santa Maria and Prunedale, California, immediately cooled, stored undisturbed in 0.45 kg clamshells at 4°C and 90–95% relative humidity for 21 dph, and photographed and phenotyped 0, 7, 14, and 21 dph (lefthand panel). EMMs for gray mold incidence (%) were estimated and plotted and exponential regressions were fit to the original phenotypic observations (right panel). R^2 estimates for goodness-of-fit of the exponential functions were 0.59 for Cabrillo, 0.22 for Monterey, 0.25 for Moxie, 0.25 for Royal Royce, and 0.50 for Valiant.

Gray mold incidence ranged from 0.0% to 2.7% among cultivars at 14 dph, a typical postharvest storage duration for LSL cultivars. The five day-neutral cultivars were screened out to 21 dph to develop insights into the postharvest storage limits for modern LSL cultivars (Figure 1). Although the fruit were still marketable at 14 dph, they became marginally marketable or unmarketable by 17–18 dph (Figure 1). We observed an exponential increase in gray mold incidence beyond 17–18 dph for every cultivar with means ranging from 10.3% to 36.7% among day-neutral cultivars at 21 dph. These studies showed that gray mold was ubiquitous and eventually rendered the fruit unmarketable but that the natural incidence of gray mold was negligible on fruit of LSL cultivars grown in coastal California within the 14 dph storage window (Figure 1; Supplementary File S2).

From common knowledge and earlier surveys of phenotypic diversity for resistance to gray mold (Gooding 1976; Barritt 1980; Lewers et al. 2012), we hypothesized that the low incidence of gray mold on commercially produced fruit of LSL cultivars might be genetically correlated with fruit firmness and other fruit quality traits affecting shelf life (Figure 2). Although phenotypic correlations have been reported (Barritt 1980), genetic correlations have not. The fruit of LSL cultivars are typically much firmer than the fruit of SSL cultivars commonly grown for local or direct-market consumption, as exemplified by Earlimiss, Madame Moutot, and Primella in the present study (Figure 2). The latter are sweeter, softer, and perish more rapidly than “Royal Royce” and other LSL cultivars under normal postharvest storage conditions (Figure 2). To explore how these phenotypic differences affect resistance to gray mold, we developed a training population ($n = 380$) for GS studies by crossing “Royal Royce,” one of the LSL cultivars assessed for natural infections (Figure 1), with four SSL cultivars (“Earlimiss,” “Madame Moutot,” “Primella,” and “Tangi”), in addition to crossing a pair of LSL

parents with differences in fruit firmness and AC (05C197P002 \times 16C108P065). These full-sib families were phenotyped for resistance to gray mold using an artificial inoculation protocol and genotyped with a 50K Axiom SNP array (Hardigan et al. 2020).

Development of a highly repeatable protocol for gray mold resistance phenotyping in strawberry

Natural infections are too inconsistent and unreliable for analyses of the genetics of resistance to gray mold in strawberry. To overcome this problem, we developed a highly repeatable artificial inoculation protocol for gray mold resistance phenotyping that involved puncturing fruit with a 3-mm probe, propagating spores of a single *B. cinerea* strain (B05.10), introducing a known concentration of spores into the wound site, and monitoring disease development on individual fruit stored undisturbed under high humidity (Figure 3). Two quantitative *B. cinerea* disease symptoms were recorded on multiple fruits harvested from training population individuals: water-soaked LD in mm and the number of dpi when EM was observed on the surface of the fruit. We found that incubating artificially inoculated fruit at 10°C and 95% humidity in the dark yielded highly repeatable results with minimal contamination from other postharvest decay pathogens. LD and EM were recorded daily from 1 to 14 dpi (Figures 3 and 4). This protocol produced highly reproducible results with repeatability estimates in the 0.66–0.83 range for LD and 0.68–0.71 range for EM (Table 1). Although critical for maximizing repeatability, this protocol produced more severe disease symptoms than those commonly observed from natural infection, especially on non-wounded fruit of firm-fruited LSL cultivars (Jarvis 1962; Petrasch et al. 2019a; Figures 1 and 3; Supplementary Figure S1).








	05C197P002	16C108P065	Royal Royce	Primella	Madame Moutot	Tangi	Earlimiss
							
Origin	UCD	UCD	UCD	The Netherlands	France	Louisiana	Mississippi
Year	2005	2016	2008	1969	1906	1972	1975
Texture	medium	firm	firm	soft	soft	medium	soft
TSS (BRIX)	high	medium	low	high	high	high	high
Titrateable Acidity	medium	low	medium	high	medium	high	high
External Color	medium	dark	medium	medium	light	medium	light

Figure 2 Fruit phenotypes for training population parents. Fruit of the parents of Royal Royce × Primella, Royal Royce × Madame Moutot, Royal Royce × Tangi, Royal Royce × Earlimiss, and 05C197P002 × 16C108P065 full-sib families. The countries and years of origin are shown for each parent. The fruit firmness categories were soft (<0.15 kg/cm²), medium (0.15–0.30 kg/cm²), and firm (>0.30 kg/cm²). The total soluble solids categories were low (< 9.0%), medium (9.0–11.0%), and high (> 11.0%). Titrateable acid (TA) concentration (%) categories were low (< 0.7%), medium (0.7–1.0%), and high (> 1.0%). External color intensity (L) categories were light (L > 41.0), medium (25.0–40.0L), and dark (<25.0L).

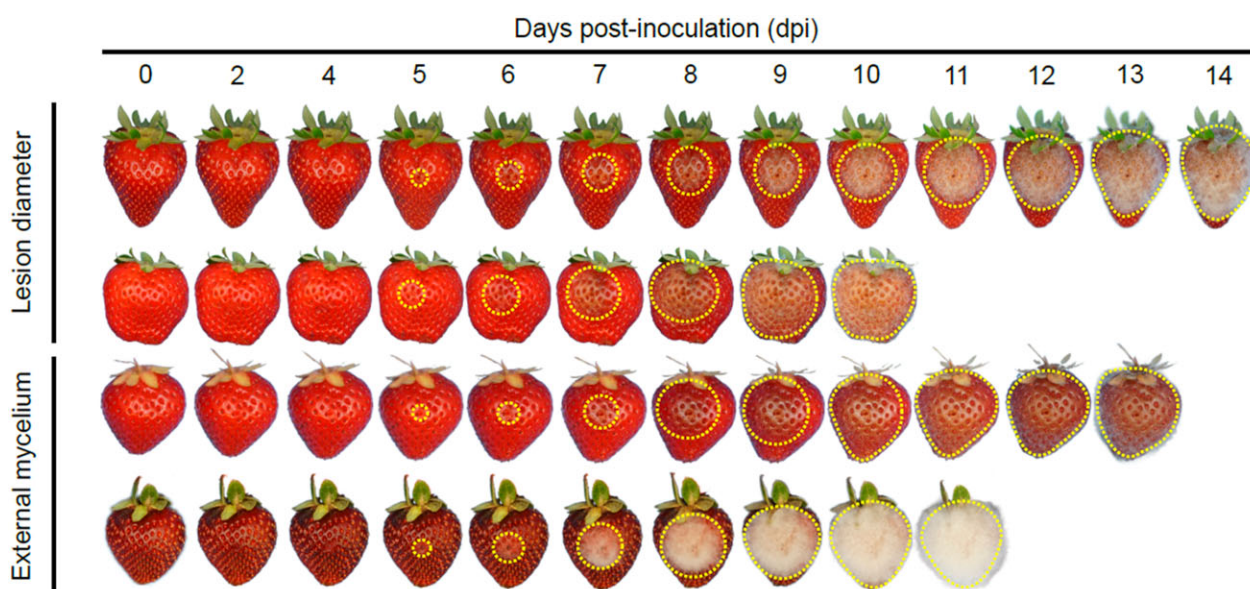


Figure 3 Postharvest progression of gray mold disease. Botrytis resistance phenotypes are shown for four multifamily training population individuals from the tails of the phenotypic distributions for LD (cm) at 8 dpi and speed of appearance of EM on the fruit surface. Fruit were artificially inoculated with the *B. cinerea* strain B05.10 and phenotyped for 0–14 dpi. The dotted yellow lines highlight approximate lesion boundaries. The 18C346P032 individual (first row) had one of the smallest LDs at 8 dpi, whereas the 18C346P030 individual (second row) had one of the largest LDs at 8 dpi. The 18C346P025 individual (third row) had one of the slowest, whereas the 18B168P085 individual (fourth row) had one of the fastest times to the appearance of mycelium on the surface of the fruit.

Genetics of resistance to gray mold in strawberry

To study the genetics of resistance to gray mold in strawberry, artificially inoculated fruit of individuals in multifamily and Royal Royce × Tangi populations were phenotyped daily for LD and EM over 14 days in cold storage (Figure 3). The speed of fungal development and symptom severity differed among individuals in both populations (Figure 4). The phenotypic extremes we observed are illustrated in time-series photographs of four individuals from the upper and lower tails of the LD and EM distributions in the multifamily population (Figure 3). Lesions became visible and had enlarged to 10.0 mm by 5 dpi in one of the most susceptible individuals (18C346P030), whereas lesions were not visible until 8 dpi and developed the slowest in one of the least susceptible individuals (18C346P032). Lesions spanned the entire fruit surface of the most susceptible individuals by 8 dpi, thereby resulting in

significant postharvest fruit deterioration and fungal decay (Figure 3). Consequently, our genetic analyses of LD were applied to phenotypes observed 8 dpi, the last day in the study that resistance phenotypes could be observed for every individual.

As expected, our analyses confirmed that resistance to gray mold is genetically complex in strawberry, a finding consistent with observations in other hosts (Lurie et al. 1997; Glazebrook 2005; Rowe and Kliebenstein 2008; Lewers et al. 2012; Corwin et al. 2016; Hanson et al. 2016; Petrasch et al. 2019a; Zhang et al. 2019; Caseys et al. 2021). Although statistically significant differences were observed among individuals for LD and EM in both populations ($P < 0.01$), every individual was susceptible and the phenotypic ranges were comparatively narrow (Figures 3 and 4). LDs were approximately normally distributed and ranged from 7.0 to 33.5 mm at 8 dpi in the multifamily population and 7.0 to

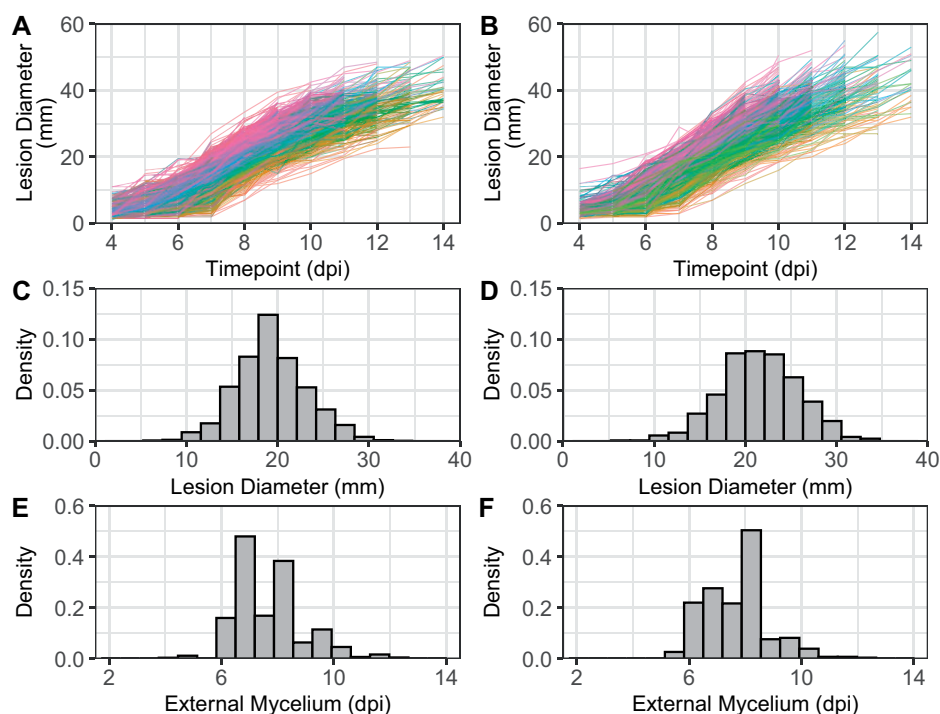


Figure 4 Distributions for gray mold resistance phenotypes. Fruit of individuals from a multifamily population ($n = 380$ individuals and $s = 1,520$ fruit) and the Royal Royce \times Tangi population ($n = 233$ individuals and $s = 1,386$ fruit) were artificially inoculated with *B. cinerea* and phenotyped 0–14 dpi for LD (mm) and the speed of emergence of EM on the surface of the fruit (dpi). (A) The EMMs for LD are shown for 0–14 dpi among 380 individuals in the multifamily population (21,280 phenotypic observations). (B) The EMMs for LD are shown for 0–14 dpi among 233 individuals in the Royal Royce \times Tangi population (9797 phenotypic observations). The disease progression curves for individuals were plotted with different colors according to their EMM ranks for LD at 8 dpi. (C, E) Phenotypic distributions for LD at 8 dpi and EM in the multifamily population. (D, F) Phenotypic distributions for LD at 8 dpi and EM in the Royal Royce \times Tangi population.

Table 1 Repeatability (r) and narrow-sense genomic heritability (h^2) estimates for gray mold LD and speed of emergence of EM

Population	Trait	\hat{r}	\hat{h}^2	
			Complete subsamples	Single subsample
Multifamily	LD	0.66	0.38	0.13
	EM	0.68	0.39	0.16
Royal Royce \times Tangi	LD	0.83	0.71	0.32
	EM	0.71	0.44	0.13

Statistics were estimated for $n = 380$ individuals and $s = 1,520$ subsamples in a multifamily population and $n = 233$ individuals and $s = 1,386$ subsamples in the Royal Royce \times Tangi population. The full-sib families in the multifamily population were Royal Royce \times Earlimiss, Royal Royce \times Madame Moutot, Royal Royce \times Primella, Royal Royce \times Tangi, and 05C197P002 \times 16C108P06. Narrow-sense genomic heritability was estimated for 100% of the subsamples ($\bar{s} = 2.9$) and for a single randomly selected subsample/individual ($\bar{s} = 1.0$) in both populations, where \bar{s} is the harmonic mean number of subsamples/individual.

34.0 mm at 8 dpi in the Royal Royce \times Tangi population (Figure 4; Supplementary Figure S2). Similarly, the speed of appearance of mycelium on the surface of the fruit (EM) was approximately normally distributed and ranged from 4.0 to 12.5 dpi in the multifamily population and 5.5 to 12.5 dpi in the Royal Royce \times Tangi population (fruit were phenotyped out to 14 dpi). The repeatabilities for LD and EM among individuals in these populations suggested that two-thirds or more of the phenotypic variation observed for gray mold resistance was genetically caused (Table 1). Narrow-sense genomic heritability estimates ranged from 0.38 to 0.71 for LD and 0.39 to 0.44 for EM, which suggested that a significant fraction of the genetic variation was additive

and thus that resistance to gray mold can be enhanced by artificial selection (Table 1).

LDs were plotted for every individual to visualize phenotypic changes in disease symptoms over time (Figure 4, A and B). The heatmap colors of the individual curves were determined from the LD EMM ranks at 8 dpi. These plots show that the speed of lesion development differed among individuals, that cross-over individual \times time interactions were negligible, and that the phenotypic changes among individuals were approximately parallel over time, all of which increased confidence in the heritability of the phenotypic differences we observed (Table 1).

Genome-wide searches failed to identify large-effect loci for LD or EM (Figure 5; Table 2). These searches included GWAS in the training populations and QTL mapping in individual full-sib families. Nine family-specific QTL with small effects were identified, eight for LD and one for EM (Table 2). None had effects large enough to warrant targeting by marker-assisted selection or inclusion as fixed effects in genomic prediction models. Although the QTL effects were small and family specific (Table 2), a few interesting candidate gene associations were identified when short QTL-associated haploblocks were searched in the reference genome for genes with biotic stress and disease resistance annotations (Supplementary File S6). A cluster of 11 tandemly duplicated genes encoding pathogenesis-related (PR) proteins were found in close proximity to the most significant SNP (AX-184469645) associated with a QTL on chromosome 4A (Table 2). These genes share sequence homology to FcPR10, an *Fragaria chiloensis* ribonuclease encoding gene previously predicted to reduce the severity of gray mold disease in strawberry (González et al. 2009, 2013). The other QTL-associated candidate genes that

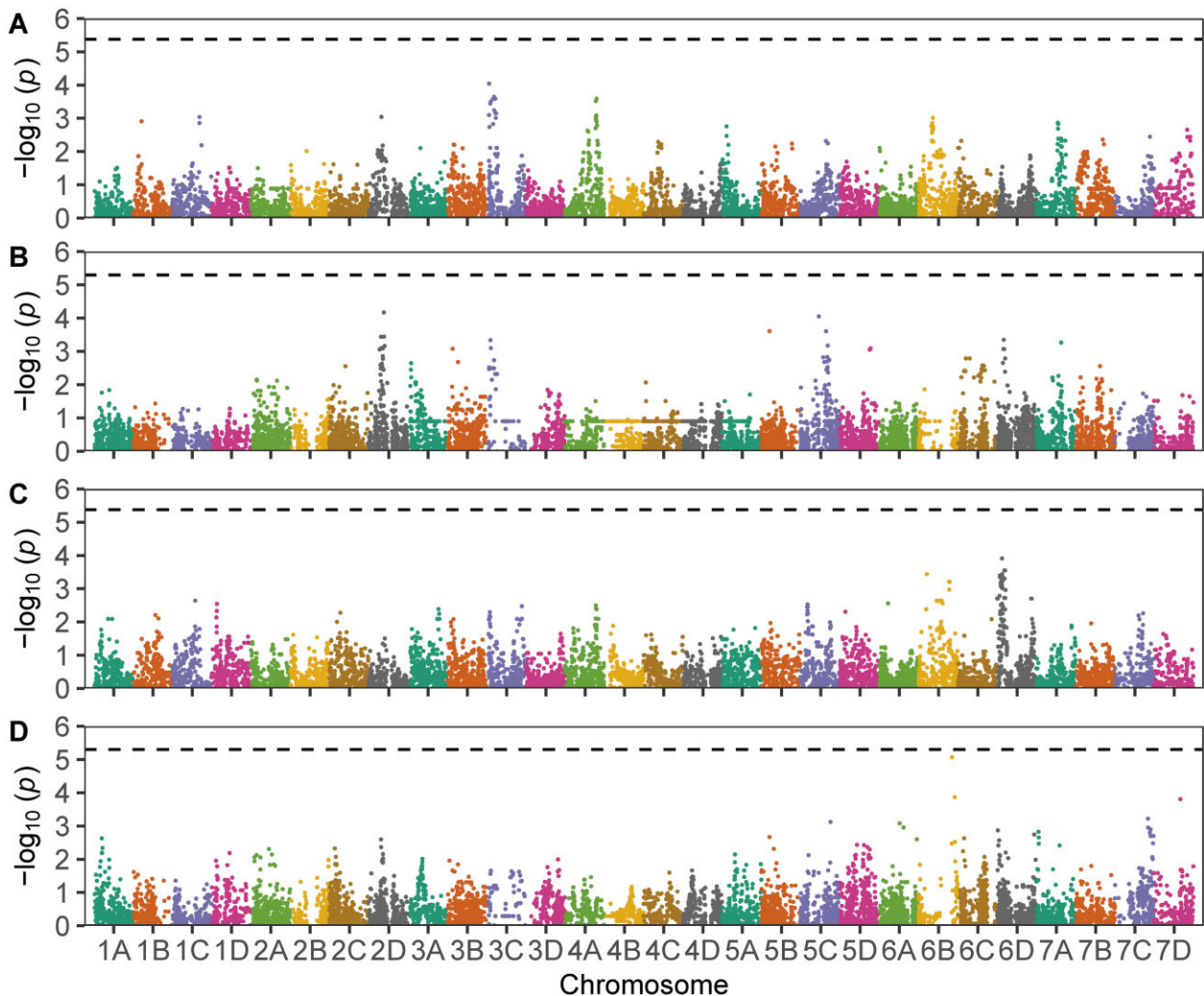


Figure 5 GWAS of gray mold resistance. Manhattan plots are shown for genome-wide scans for marker-trait associations for LD at 8 dpi in the multifamily (A), LD at 8 dpi in the Royal Royce \times Tangi (B), speed of emergence of EM on the surface of the fruit in the multifamily (C), and EM in the Royal Royce \times Tangi (D) populations. The individuals in both populations were genotyped with a 50K Axiom SNP array. The analyses were done using the “Camarosa” reference genome (Edger et al. 2019) with physical positions of SNP markers ascertained by (Hardigan et al. 2020) using the chromosome nomenclature of (Hardigan et al. 2021). Horizontal dashed lines identify the genome-wide Bonferroni significance threshold.

might warrant further study encode peroxidases (chromosome 7D; Mb 576-2709) reported to modulate reactive oxygen species levels and inhibit fungal growth during *B. cinerea* infections (Cantu et al. 2008, 2009; Tomas-Grau et al. 2018) and transcription factors reported to signal pathogen-triggered immunity, e.g., WRKY and AP2/ERF (chromosome 3B; Mb 13,870–15,400; Gutterson and Reuber 2004; Bigeard et al. 2015), that might target pathogenicity factors, e.g., chitinases (van Schie and Takken 2014) and protease inhibitors (Hermosa et al. 2006; Billon-Grand et al. 2012). While these genes are worthwhile candidates for further study (González et al. 2009, 2013; Petrasch et al. 2019a), the effects of the associated QTL were too small and insignificant for direct selection (Table 2). This was, nevertheless, a first attempt to identify loci underlying resistance to *B. cinerea* in strawberry through a genome-wide search for genotype-to-phenotype associations in the octoploid genome (Supplementary File S6).

Royal Royce, the firm-fruited LSL parent, was more resistant to gray mold than the soft-fruited SSL parents (phenotypic distributions and parent EMMs for each full-sib family are shown in Supplementary Figure S2). Lesions were smaller and mycelium appeared later in Royal Royce than the other parents (resistance

increased as LD decreased and EM increased). Royal Royce was the more resistant parent for both traits in the four full-sib families with that parent (Figure 2; Supplementary Figure S2). For the 05C197P002 \times 16C108P065 full-sib family, 05C197P002 was more resistant than 16C108P065 for LD and vice versa for EM. The LD and EM differences were highly significant ($P \leq 0.01$) with individuals transgressing the phenotypic ranges of the parents (Supplementary Figure S2). Transgressive segregation was primarily bidirectional for both traits; however, the EM distributions for Royal Royce \times Tangi and 05C197P002 \times 16C108P065 were right-skewed toward more resistance (slower EM emergence) and lacked individuals in the lower tails distal to the more susceptible parent (Supplementary Figure S2). These results suggested that favorable alleles were transmitted by both parents for both traits and that favorable alleles for different loci segregated in most of the families.

Genomic prediction accuracies varied between populations and symptoms

Genomic prediction accuracies for different WGR methods ranged from 0.28 to 0.47 for LD and 0.37 to 0.59 for EM when

Table 2 Summary statistics for QTL affecting gray mold resistance^a in strawberry

Population	SNP marker ^b	Chromosome ^c	Position (Mb) ^d	Contrast ^e	Effect	LOD ^f	Allele ^g
LD (mm)							
05C197P002 × 16C108P065	AX-184345814	7D	0.0	AA-AB	-3.48	4.03	05C197P002
Royal Royce × Primella	AX-184496623	3B	105.0	BB-AB	2.49	3.61	Royal Royce
Royal Royce × Primella	AX-184685020	5C	88.7	AA-AB	-0.87	3.70	Royal Royce
Royal Royce × Earlimiss	AX-184026159	3C	24.2	AA-AB	-2.79	5.36	Royal Royce
Royal Royce × Earlimiss	AX-184469645	4A	101.6	AA-AB	2.52	4.26	Earlimiss
Royal Royce × Tangi	AX-184718804	3C	52.8	BB-AB	1.92	4.21	Royal Royce
Royal Royce × Tangi	AX-184031508	5A	0.0	BB-AB	1.92	4.56	Royal Royce
Royal Royce × Tangi	AX-184266150	7C	21.7	AA-AB	1.82	3.70	Tangi
EM (dpi)							
Royal Royce × Tangi	AX-184857528	5C	93.1	BB-AB	0.48	4.03	Tangi

^a LD and the speed of emergence of EM on the surface of the fruit were recorded daily from 0 to 14 dpi. QTL statistics are shown for LD at 8 dpi, the last day that none of the fruit had perished.

^b Alphanumeric names for SNP markers on the 50K Axiom SNP array Hardigan et al. (2020) with the largest effects (largest LOD score) for a particular QTL.

^c Chromosome numbers follow the nomenclature proposed by Hardigan et al. (2021) with letters designating subgenomes (A–D) and numbers designating homoeologous chromosomes (1–7).

^d The physical positions of SNP markers were ascertained by Hardigan et al. (2020) from alignments of SNP probe sequences to the *F. × ananassa* “Camarosa” reference genome (Edger et al. 2019).

^e SNP marker genotypes were coded AA, AB, and BB where A is the allele transmitted by the parent shown on the left in the pedigree and B is the allele transmitted by the parent shown on the right in the pedigree. Contrasts were estimated for each SNP marker as the difference between EMMs for genotypes. The AA-AB contrast compared EMMs between AA homozygotes and AB heterozygotes, whereas the BB-AB contrast compared EMMs between BB homozygotes and AB heterozygotes.

^f Logarithm of the odds (LOD) scores for SNP marker-QTL associations that exceeded statistical thresholds estimated by permutation.

^g The parent that transmitted the favorable allele. The favorable allele for LD decreased the EMM, whereas the favorable allele for EM increased the EMM.

Table 3 Genomic prediction accuracy for gray mold resistance

Population ^a	WGR method ^b	Genomic prediction accuracy	
		Complete subsample cross-validation ^c	Single subsample cross-validation ^d
LD (mm)			
Multifamily	G-BLUP	0.33	0.17
	RKHS	0.33	0.19
	SVM	0.28	0.17
Royal Royce × Tangi	GBLUP	0.52	0.56
	RKHS	0.59	0.57
	SVM	0.59	0.58
EM (dpi)			
Multifamily	G-BLUP	0.47	0.35
	RKHS	0.47	0.34
	SVM	0.44	0.40
Royal Royce × Tangi	G-BLUP	0.37	0.36
	RKHS	0.42	0.34
	SVM	0.40	0.35

^a Statistics were estimated from analyses of $n = 380$ individuals and $s = 1,520$ subsamples in a multifamily population and $n = 233$ individuals and $s = 1,386$ subsamples in the Royal Royce × Tangi population. The full-sib families in the multifamily population were Royal Royce × Earlimiss, Royal Royce × Madame Moutot, Royal Royce × Primella, Royal Royce × Tangi, and 05C197P002 × 16C108P065.

^b GEBVs were estimated using G-BLUP, RKHS regression, and SVM.

^c GEBVs and genomic prediction accuracies were estimated from 100% of the subsamples/individual by cross-validation with 1000 permutations using 80% of the individuals for training and 20% of the individuals for prediction, where the harmonic mean number of subsamples/individual (\bar{s}) = 2.9.

^d Genomic prediction accuracy was estimated from a single randomly selected subsample/individual by cross-validation with 1000 permutations using 80% of the individuals for training and 20% of the individuals for prediction.

estimated by cross-validation from 100% of the subsamples (Table 3; Supplementary Figure S3). The differences in accuracy among WGR methods for each trait-population combination ranged from 0.00 to 0.07. RKHS produced the highest accuracy for two of the trait-population combinations and was equal in accuracy to G-BLUP for the other two trait-population combinations. SVM often performed intermediate to both G-BLUP and RKHS. The prediction accuracy was greater for LD than EM in the Royal Royce × Tangi population, whereas the reverse was observed in the multifamily population. Using cross-validation with 100% of the subsamples, clear differences in prediction accuracy and shrinkage were observed between disease symptoms within and between populations (Table 3; Supplementary Figure S3). The prediction accuracy for LD was markedly different between the

multifamily and Royal Royce × Tangi populations. The GEBV range for LD in the multifamily population was half as wide (15.5–22.8) and the kernel density was flatter and more vertical than that observed in the Royal Royce × Tangi population (13.3–27.4; Supplementary Figure S3). Notably, the LD phenotypes of the most resistant individuals in the RR × Tangi population (those with the smallest LD means) were well predicted. Their EM phenotypes, however, were not as well predicted—the GEBV range for EM (6.8–9.2) was half that of the phenotypic range (5.5–10.7) and the kernel density distribution was flatter and more vertical (Supplementary Figure S3).

One of the challenges of breeding for resistance to gray mold and other postharvest traits is phenotyping throughput. Collectively, 2563 fruit were harvested and individually stored,

tracked, and phenotyped in our study (Figure 4). Our expectation was that multiple fruit/individual was needed to more accurately estimate EMMs and GEBVs and nominally increase heritability. To assess the effect of subsamples on prediction accuracy and explore the feasibility of applying selection for resistance to gray mold from a single subsample/individual, GEBVs and prediction accuracies were estimated from a single randomly selected subsample/individual. We observed a significant decrease in narrow-sense genomic heritability for LD and EM in the single subsample analyses, *e.g.*, \hat{h}^2 decreased from 0.38 to 0.13 for LD and 0.39 to 0.16 for EM in the multifamily population (Table 1). Naturally, prediction accuracies plummeted in the single subsample analyses too (Table 3; Supplementary Figure S3). This is clearly illustrated by the kernel density distributions for GS accuracy estimated for G-BLUP, RKHS, and SVM by cross-validation with a single subsample/individual (Supplementary Figure S3). GEBV ranges were narrower and kernel density distributions were flatter and more vertical for the single subsample vs multiple subsample analyses for LD and EM in both populations (Supplementary Figure S3). Hence, we concluded that breeding values cannot be accurately predicted without subsampling fruit.

Gray mold resistance traits were genetically correlated with shelf life-associated fruit quality traits

One of our working hypotheses was that selection for increased fruit firmness and other shelf life-associated fruit quality traits pleiotropically decreased susceptibility to gray mold in strawberry. The additive genetic correlations support this hypothesis and highlight between family differences driven by breeding history, the phenotypic diversity of the parents, and transgressive segregation (Figures 3 and 6; Supplementary Figure S2). The pairwise breeding value distributions further highlight the family structure and phenotypic diversity within and among families. The fruit size, firmness, and TA by LD and EM breeding value distributions for the only elite \times elite family in our study (05C197P002 \times 16C108P065) were distinct from the four elite \times exotic families (Figure 6, A–D and I and J).

LD and EM were weakly negatively genetically correlated ($\hat{r}_A = -0.21$) and weakly to strongly genetically correlated with fruit quality traits in directions predicted by our hypotheses. Because gray mold resistance increases as LD decreases and EM increases, signs of the additive genetic correlations have different interpretations for LD and EM and can be antagonistic or synergistic. The interpretation depends on the specific phenotypes targeted for a particular market, *e.g.*, SSL vs LSL. LD was negatively genetic correlated with titratable acidity ($\hat{r}_A = -0.41$) and positively genetically correlated with pH ($\hat{r}_A = 0.41$); hence, LD increased as titratable acidity decreased and pH increased (Figure 6, I and J). The effect of titratable acidity on resistance phenotypes was the motivation for screening additional individuals from the Royal Royce \times Tangi family, which had a significant genetic variation for TA and yielded more accurate genomic predictions for LD than were observed in the multifamily population (Supplementary Figure S3). EM was more strongly positively genetically correlated with fruit size and firmness than LD and negatively genetically correlated with total soluble solids (Figure 6). EM increased (disease resistance increased) as BRIX decreased and fruit size and firmness increased. Hence, we found that mycelium developed faster on softer, sweeter, and smaller fruit than

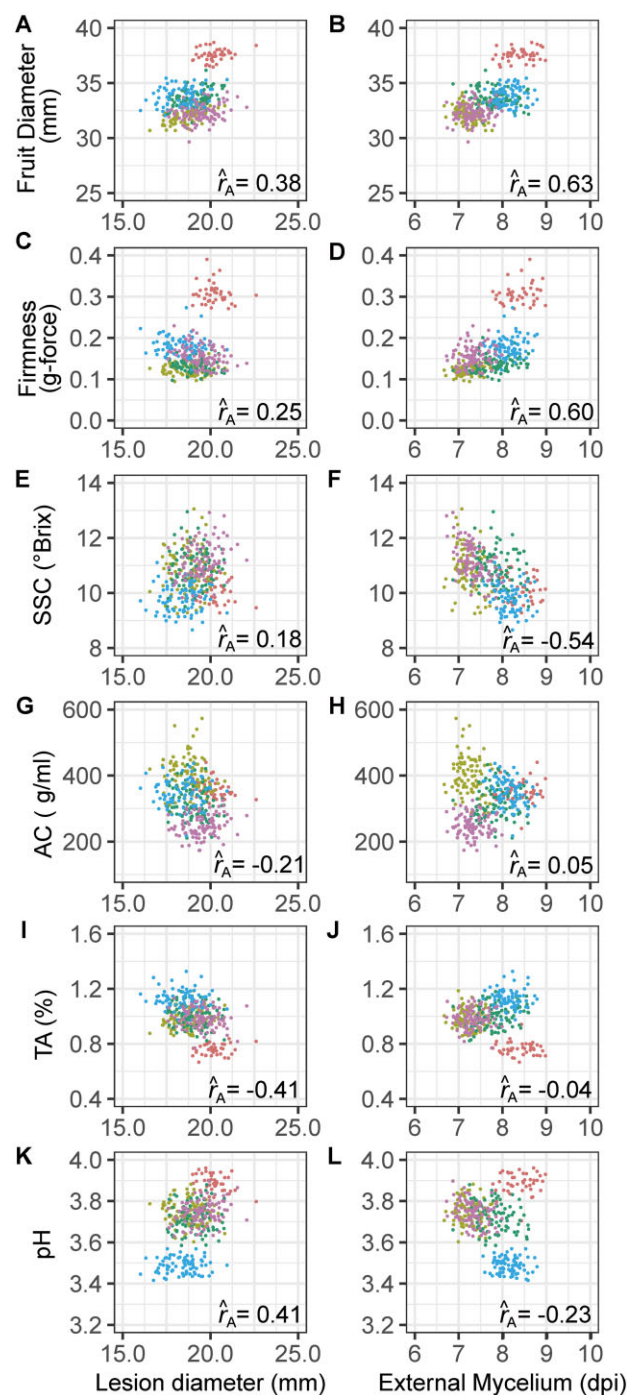


Figure 6 Additive genetic correlations (\hat{r}_A). Scatter plots are shown for G-BLUP estimates of GEBVs for gray mold resistance and fruit quality traits among 380 individuals in a multifamily training population. The individual families are Royal Royce \times Primella (olive), Royal Royce \times Madame Moutot (green), Royal Royce \times Tangi (blue), Royal Royce \times Earlimiss (magenta), and 05C197P002 \times 16C108P065 (coral). The abbreviations for fruit quality traits are SSC, soluble solids content; AC, anthocyanin content; TA, titratable acidity.

firmer, less sweet, and larger fruit, as is typical of Royal Royce and other modern LSL cultivars (Figures 1 and 2).

Finally, LD was weakly negatively genetically correlated with AC, whereas EM was uncorrelated with AC (Figure 6, G and H).

Although the additive genetic correlation we observed between LD and AC was in the direction predicted by previous studies in strawberry and tomato (Jersch et al. 1989; Hébert et al. 2002; Bassolino et al. 2013; Zhang et al. 2013), LD only slightly decreased as AC increased (Figure 6).

Breeding for enhanced resistance to gray mold in strawberry

Breeding for resistance to necrotrophic pathogens has been challenging in plants (Finkers et al. 2007a, 2007b; Williamson et al. 2007; Petrasch et al. 2019a; Lorang 2019; Delplace et al. 2020). The mechanisms of resistance to necrotrophic pathogens are more subtle, quantitative, and complex than those commonly observed for biotrophic pathogens that trigger pathogen-associated molecular pattern-triggered-immunity and effector-triggered immunity (Glazebrook 2005; Jones and Dangl 2006; Jones et al. 2016; Saijo et al. 2018; Lorang 2019; Zhang et al. 2019; Caseys et al. 2021). Our findings were well aligned with previous findings in other *B. cinerea* hosts and shed light on the genetic complexity of resistance to gray mold in strawberry. Where do we go from here? We are skeptical that significant genetic gains can be achieved for gray mold resistance across the complete shelf life spectrum in strawberry but are confident that postharvest gray mold incidence can be minimized but obviously not eliminated in LSL populations. This conclusion seems well aligned with previous findings in strawberry and other hosts of this pathogen (Finkers et al. 2007a, 2007b; Rowe and Kliebenstein 2008; Lewers et al. 2012). Because several fruit quality traits pleiotropically affect gray mold resistance in strawberry, the challenge is exponentially greater when breeding for markets where softer fruits with elevated sugars are preferred and LSL phenotypes are neither necessary nor preferred (Figures 1, 2 and 6). However, for markets where LSL cultivars are essential, direct selection for the requisite fruit quality traits seems to confer sufficient resistance to gray mold to ensure marketability under normal postharvest storage conditions and timelines, especially for fruit produced in coastal California and other arid and semi-arid environments with low humidity and rainfall (Figure 1; Supplementary Figure S1). Although we only sampled 12 coastal California environments (six locations \times two harvests/location) to estimate the natural incidence of *B. cinerea* among eight LSL cultivars, we suspect that deeper sampling will confirm our findings.

There are open questions to be addressed and were limitations to our study. First, we did not screen diverse germplasm to identify sources of resistance to gray mold. As our study and others have shown, strong sources of resistance to this pathogen may not exist (Chandler et al. 2006; Seijo et al. 2008; Lewers et al. 2012; Bestfleisch et al. 2015). The narrow-sense heritability estimates and genomic prediction results for LD and EM in the present study suggest that a deeper exploration of genetic diversity, while challenging, seems worthwhile (Table 1; Supplementary Figure S3). The association between resistance and titratable acidity seems to be particularly promising and worthy of further study (Figure 6), particularly if increased acidity is offset by increased sugars to achieve a palatable sugar: acid balance.

Second, the parents for this study were selected to assess the effects of fruit quality and shelf life-associated traits on gray mold disease development (Figure 2), not for known intrinsic differences in gray mold resistance that are genetically uncorrelated with fruit quality and shelf life phenotypes. The pleiotropic effects of shelf life-associated fruit quality traits on gray mold susceptibility appear to be inescapable (Figure 6). Our results suggest that resistance can be increased by selecting for

increased titratable acidity and firmness and decreased sugars but these phenotypes profoundly affect flavor and cannot be manipulated in a vacuum (Zorrilla-Fontanesi et al. 2011; Diamanti et al. 2012; Lerceteau-Köhler et al. 2012; Verma et al. 2017). Without more extensive germplasm screening, the data needed to guide the selection of parents for future genetic studies are lacking.

Third, the natural incidence of gray mold was only explored in the present study for LSL cultivars commercially grown in California (Figure 1). Highly perishable short- and medium-shelf life cultivars, as typified by the heirloom cultivars (parents) we screened (Figure 2), are challenging to grow and phenotype in such studies because they typically have low yields, are easily bruised and wounded, and cannot be harvested and handled with the same robustness as commercially important LSL cultivars. Nevertheless, a study of the natural incidence of gray mold among individuals spanning the shelf life spectrum could shed further light on genetic correlations between fruit quality and gray mold resistance phenotypes and possibly identify sources of favorable alleles underlying intrinsic resistance that are uncorrelated with fruit quality traits, e.g., biochemical phenotypes triggered by defense mechanisms (Diaz et al. 2002; Glazebrook 2005; van Kan 2006; Williamson et al. 2007; Veloso and van Kan 2018; Lorang 2019; Petrasch et al. 2019a). Because gray mold disease symptoms from artificial inoculation protocols are typically harsher than those observed from natural infections of non-wounded fruit (Figures 1 and 3), a deeper exploration of the natural incidence of gray mold seems warranted in strawberry, perhaps by simulating rainfall in field experiments through overhead irrigation or other practices to increase the uniformity and incidence of natural infection.

Our results suggest that phenotypic or GS could be effective for gray mold resistance but only in certain populations and only when selection for genetically correlated traits does not antagonistically reduce genetic gains for gray mold resistance phenotypes (Table 3; Supplementary Figure S3). Genetic gains for gray mold resistance are affected by shelf life-related traits through additive genetic correlations and could be reversed by simultaneous selection for fruit quality and shelf life traits that antagonistically pleiotropically affect gray mold resistance phenotypes (Figure 6). Genetic variation for fruit quality traits strongly affected the phenotypic differences we observed for LD and EM. Most importantly, the fruit quality traits associated with enhanced flavor were antagonistically genetically correlated with gray mold resistance phenotypes (Figure 6).

Cross-validation of genomic predictions in the present study shed light on the complexity of genetic mechanisms underlying gray mold resistance phenotypes and highlighted the challenges inherent in breeding for increased resistance to gray mold in strawberry (Table 3; Supplementary Figure S3). The three WGR methods we applied to the prediction problem strongly shrunk breeding values to the population mean for LD in the multifamily and EM in the Royal Royce \times Tangi populations. Such shrinkage is typical for moderately heritable complex diseases in plants (Rutkoski et al. 2011, 2014; Poland and Rutkoski 2016).

The prospects for identifying superior genotypes through GS were greater for LD in the Royal Royce \times Tangi population and EM in the multifamily population than vice versa. Whether applying phenotypic or GS, the probability of selecting superior genotypes can be exceedingly low when breeding for resistance to genetically complex diseases in plants (Poland and Rutkoski 2016; Crossa et al. 2017; Voss-Fels et al. 2019). Nevertheless, with cost-effective genome-wide genotyping, GS has the potential to

increase genetic gains by increasing the number of selection candidates that can be screened per unit of time and space (Poland and Rutkoski 2016; Crossa et al. 2017). Even in the small populations we studied ($n=380$ and $n=233$), nearly 20,000 phenotypic observations were collected to quantitatively assess resistance to gray mold, which included image analyses at each postinoculation time point (Figure 4). The phenotyping throughput needed to effectively evaluate postharvest traits in strawberry can be limiting, particularly when multiple harvests are factored into the equation, e.g., day-neutral cultivars are typically harvested twice weekly over a period of six to eight months in coastal California. Because the progression of disease symptoms was continuous and genotype \times storage time interactions were negligible (Figure 4), phenotyping throughput can be increased by employing a response surface experiment design, e.g., by phenotyping fruit at three equally spaced time points spanning the range needed to estimate response curves and accurately predict LD and EM phenotypes (Hill and Hunter 1966; Khuri and Mukhopadhyay 2010). This is precisely the sort of breeding problem where genomic prediction methods have the greatest potential utility and applicability (Heffner et al. 2010; Jannink et al. 2010; Lin et al. 2014), despite the complexity of the underlying genetic mechanisms and variable prediction accuracies across populations, which nevertheless affect phenotypic and GS equally (Table 3; Supplementary Figure S3).

Data availability

Genotypic, phenotypic, and other supplemental data files, figures, and tables are centrally available at <https://figshare.com>. Supplementary File S1 is a text file with a custom macro developed to process photographic images of strawberry fruit using ImageJ, a “public domain Java image processing program” (<https://imagej.nih.gov/ij/index.html>). Supplementary File S2 stores 50K Axiom SNP array genotypic data for individuals in the training populations (five full-sib families). Supplementary File S3 stores the phenotypic data for the training populations. Custom R and PERL scripts developed for genetic mapping analyses are stored in Supplementary File S4. Supplementary File S5 stores chromosome numbers, genetic and physical coordinates for SNP markers, and other information for the 10 parent-specific genetic maps constructed for each of the five full-sib families, in addition to summary statistics for each genetic map, e.g., number of mapped SNP marker loci and map length (cM). Supplementary File S6 stores information on candidate genes linked to gray mold resistance QTL with physical addresses and genome annotations from the *F. \times ananassa* “Camarosa” v1.0 reference genome (Edger et al. 2019). The latter is available at the Genome Database for Rosaceae (https://www.rosaceae.org/species/fragaria_x_ananassa/genome_v1.0.a1). Supplementary File S7 stores the EMMs and GEBVs for gray mold resistance and fruit quality phenotypes among 380 individuals in a multifamily training population and 233 individuals in the Royal Royce \times Tangi population. Supplementary Figure S1 displays time-series photographs of fruit of the LSL summer-plant cultivars “UCD Finn” and “UCD Mojo” at 0, 7, and 14 days of postharvest storage. Supplementary Figure S2 displays the distributions and parent EMMs for gray mold resistance phenotypes within full-sib families. Supplementary Figure S3 displays kernel density plots for genomic prediction accuracies estimated by cross-validation for G-BLUP, RKHS, and SVM.

Supplementary material is available at figshare: <https://doi.org/10.25387/g3.14732073>

Acknowledgments

The authors thank N.N.H. and O.W. for assisting in disease assessments and N.V.D.P., B.C., and E.G. for assisting in fruit harvests.

Funding

This research was supported by grants to S.J.K. from the United States Department of Agriculture (<http://dx.doi.org/10.13039/100000199>) National Institute of Food and Agriculture (NIFA) Specialty Crops Research Initiative (# 2017-51181-26833), California Strawberry Commission (<http://dx.doi.org/10.13039/100006760>), and the University of California, Davis (<http://dx.doi.org/10.13039/100007707>) and B.B.-U. from UCD College of Agricultural and Environmental Sciences and the Department of Plant Sciences start-up funds. These funding sources supported the dissertation research of S.P.

Conflicts of interest

The authors declare that there is no conflict of interest.

Literature cited

- Barritt B. 1980. Resistance of strawberry clones to *Botrytis* fruit rot. *J Am Soc Hortic Sci.* 105:160–164.
- Bassolino L, Zhang Y, Schoonbeek H-J, Kiferle C, Perata P, et al. 2013. Accumulation of anthocyanins in tomato skin extends shelf life. *New Phytol.* 200:650–655.
- Bates D, Mächler M, Bolker B, Walker S. 2015. Fitting linear mixed-effects models using lme4. *J Stat Softw.* 67:1–48.
- Bestfleisch M, Luderer-Pflimpfl M, Höfer M, Schulte E, Wünsche J, et al. 2015. Evaluation of strawberry (*Fragaria L.*) genetic resources for resistance to *Botrytis cinerea*. *Plant Pathol.* 64:396–405.
- Bigéard J, Colcombet J, Hirt H. 2015. Signaling mechanisms in pattern-triggered immunity (PTI). *Mol Plant.* 8:521–539.
- Billon-Grand G, Rasclé C, Droux M, Rollins JA, Poussereau N. 2012. pH modulation differs during sunflower cotyledon colonization by the two closely related necrotrophic fungi *Botrytis cinerea* and *Sclerotinia sclerotiorum*. *Mol Plant Pathol.* 13:568–578.
- Blanco-Ulate B, Labavitch JM, Vincenti E, Powell ALT, Cantu D. 2016a. Hitting the wall: plant cell walls during *Botrytis cinerea* infections. In: S Fillinger, Y Elad, editors. *Botrytis – The Fungus, the Pathogen and its Management in Agricultural Systems*. Cham: Springer International Publishing. p. 361–386.
- Blanco-Ulate B, Vincenti E, Cantu D, Powell AL. 2016b. Ripening of tomato fruit and susceptibility to *Botrytis cinerea*. In: Fillinger S, Elad Y, editors. *Botrytis – The Fungus, the Pathogen and its Management in Agricultural Systems*. Cham: Springer International Publishing. p. 387–412.
- Broman KW, Wu H, Sen S, Churchill GA. 2003. R/qtl: QTL mapping in experimental crosses. *Bioinformatics.* 19:889–890.
- Büttner P, Koch F, Voigt K, Quidde T, Risch S, et al. 1994. Variations in ploidy among isolates of *Botrytis cinerea*: implications for genetic and molecular analyses. *Curr Genet.* 25:445–450.
- Cantu D, Blanco-Ulate B, Yang L, Labavitch JM, Bennett AB, et al. 2009. Ripening-regulated susceptibility of tomato fruit to *Botrytis cinerea* requires NOR but not RIN or ethylene. *Plant Physiol.* 150:1434–1449.
- Cantu D, Vicente AR, Greve L, Dewey F, Bennett A, et al. 2008. The intersection between cell wall disassembly, ripening, and fruit

- susceptibility to *Botrytis cinerea*. Proc Natl Acad Sci U S A. 105: 859–864.
- Caseys C, Shi G, Soltis N, Gwinner R, Corwin J, et al. 2021. Quantitative interactions: the disease outcome of *Botrytis Cinerea* across the plant kingdom. G3 (Bethesda). 11:jkab175.
- Chandler CK, Mertely JC, Peres N. 2006. Resistance of selected strawberry cultivars to anthracnose fruit rot and *Botrytis* fruit rot. Acta Hort. 708:123–126.
- Churchill GA, Doerge RW. 1994. Empirical threshold values for quantitative trait mapping. Genetics. 138:963–971.
- Corwin JA, Copeland D, Feusier J, Subedy A, Eshbaugh R, et al. 2016. The quantitative basis of the arabidopsis innate immune system to endemic pathogens depends on pathogen genetics. PLoS Genet. 12:e1005789.
- Cosseboom SD, Ivors KL, Schnabel G, Bryson PK, Holmes GJ. 2019. Within-season shift in fungicide resistance profiles of *Botrytis cinerea* in California strawberry fields. Plant Dis. 103:59–64.
- Crossa J, Pérez-Rodríguez P, Cuevas J, Montesinos-López O, Jarquín D, et al. 2017. Genomic selection in plant breeding: methods, models, and perspectives. Trends Plant Sci. 22:961–975.
- de Los Campos G, Gianola D, Rosa GJ, Weigel KA, Crossa J. 2010. Semi-parametric genomic-enabled prediction of genetic values using reproducing kernel hilbert spaces methods. Genet Res (Camb). 92:295–308.
- Dean R, Van Kan JA, Pretorius ZA, Hammond-Kosack KE, Pietro AD, et al. 2012. The top 10 fungal pathogens in molecular plant pathology. Mol Plant Pathol. 13:414–430.
- Delplace F, Huard-Chauveau C, Dubiella U, Khafif M, Alvarez E, et al. 2020. Robustness of plant quantitative disease resistance is provided by a decentralized immune network. Proc Natl Acad Sci U S A. 117:18099–18109.
- Dewey FM, Grant-Downton R. 2016. *Botrytis* – biology, detection and quantification. In: S Fillinger, Y Elad, editors. *Botrytis – The Fungus, the Pathogen and its Management in Agricultural Systems*. Cham: Springer International Publishing. p. 17–34.
- Diamanti J, Capocasa F, Balducci F, Battino M, Hancock J, et al. 2012. Increasing strawberry fruit sensorial and nutritional quality using wild and cultivated germplasm. PLoS One. 7:e46470.
- Diaz J, ten Have A, van Kan JA. 2002. The role of ethylene and wound signaling in resistance of tomato to *Botrytis cinerea*. Plant Physiol. 129:1341–1351.
- do Nascimento Nunes MC. 2015. Correlations between subjective quality and physicochemical attributes of fresh fruits and vegetables. Postharvest Biol Technol. 107:43–54.
- Edger PP, Poorten TJ, VanBuren R, Hardigan MA, Colle M, et al. 2019. Origin and evolution of the octoploid strawberry genome. Nat Genet. 51:541–547.
- Elad Y, Evensen K. 1995. Physiological aspects of resistance to *Botrytis cinerea*. Phytopathology. 85:637–643.
- Elad Y, Pertot I, Prado AMC, Stewart A. 2016. Plant hosts of *Botrytis* spp. In: Fillinger, S., Elad Y. (eds.) *Botrytis – The Fungus, the Pathogen and Its Management in Agricultural Systems*. Cham: Springer. p. 413–486.
- Endelman JB. 2011. Ridge regression and other kernels for genomic selection with R package rrBLUP. Plant Genome. 4:250–255.
- Finkers R, Bai Y, van den Berg P, van Berloo R, Meijer-Dekens F, et al. 2008. Quantitative resistance to *Botrytis cinerea* from *Solanum neorickii*. Euphytica. 159:83–92.
- Finkers R, van den Berg P, van Berloo R, Ten Have A, van Heusden AW, et al. 2007a. Three QTLs for *Botrytis cinerea* resistance in tomato. Theor Appl Genet. 114:585–593.
- Finkers R, van Heusden AW, Meijer-Dekens F, van Kan JA, Maris P, et al. 2007b. The construction of a *Solanum habrochaites* LYC4 introgression line population and the identification of QTLs for resistance to *Botrytis cinerea*. Theor Appl Genet. 114:1071–1080.
- Glazebrook J. 2005. Contrasting mechanisms of defense against biotrophic and necrotrophic pathogens. Annu Rev Phytopathol. 43: 205–227.
- González G, Fuentes L, Moya-León MA, Sandoval C, Herrera R. 2013. Characterization of two PR genes from *Fragaria chiloensis* in response to *Botrytis cinerea* infection: a comparison with *Fragaria × ananassa*. Physiol Mol Plant Pathol. 82:73–80.
- González G, Moya M, Sandoval C, Herrera R. 2009. Genetic diversity in Chilean strawberry (*Fragaria chiloensis*): differential response to *Botrytis cinerea* infection. Span J Agric Res. 7:886–895.
- Gooding H. 1976. Resistance to mechanical injury and assessment of shelf life in fruits of strawberry (*Fragaria × ananassa*). Hortic Res. 16:71–82.
- Gutterson N, Reuber TL. 2004. Regulation of disease resistance pathways by AP2/ERF transcription factors. Curr Opin Plant Biol. 7: 465–471.
- Haley CS, Knott SA. 1992. A simple regression method for mapping quantitative trait loci in line crosses using flanking markers. Heredity (Edinb). 69:315–324.
- Hanson P, Lu S-F, Wang J-F, Chen W, Kenyon L, et al. 2016. Conventional and molecular marker-assisted selection and pyramiding of genes for multiple disease resistance in tomato. Sci Hortic. 201:346–354.
- Hardigan MA, Feldmann MJ, Lorant A, Bird KA, Famula R, et al. 2019. Genome synteny has been conserved among the octoploid progenitors of cultivated strawberry over millions of years of evolution. Front Plant Sci. 10:1789.
- Hardigan MA, Lorant A, Pincot DD, Feldmann MJ, Famula RA, et al. 2021. Unraveling the complex hybrid ancestry and domestication history of cultivated strawberry. Mol Biol Evol. 38:2285–2305.
- Hébert C, Charles M, Gauthier L, Willemot C, Khanizadeh S, et al. 2002. Strawberry proanthocyanidins: biochemical markers for *Botrytis cinerea* resistance and shelf-life predictability. Acta Hort. 567:659–662.
- Heffner EL, Lorenz AJ, Jannink J-L, Sorrells ME. 2010. Plant breeding with genomic selection: gain per unit time and cost. Crop Sci. 50: 1681–1690.
- Hermosa M, Turra D, Fogliano V, Monte E, Lorito M. 2006. Identification and characterization of potato protease inhibitors able to inhibit pathogenicity and growth of *Botrytis cinerea*. Physiol Mol Plant Pathol. 68:138–148.
- Hill WJ, Hunter WG. 1966. A review of response surface methodology: a literature survey. Technometrics. 8:571–590.
- Jannink J-L, Lorenz AJ, Iwata H. 2010. Genomic selection in plant breeding: from theory to practice. Brief Funct Genom. 9:166–177.
- Jarvis W. 1962. The infection of strawberry and raspberry fruits by *Botrytis cinerea* Fr. Ann Appl Biol. 50:569–575.
- Jersch S, Scherer C, Huth G, Schlösser E. 1989. Proanthocyanidine als Ursache der Quieszenz von *Botrytis cinerea* in unreifen Erdbeerfrüchten. Z Pflanzenk Pflanzen. 96:365–378.
- Jones JD, Dangl JL. 2006. The plant immune system. Nature. 444: 323–329.
- Jones JD, Vance RE, Dangl JL. 2016. Intracellular innate immune surveillance devices in plants and animals. Science. 354:aaf6395-1--aaf6395-8.
- Khuri AI, Mukhopadhyay S. 2010. Response surface methodology. Wires Comp Stat. 2:128–149.

- Legard D, Chandler C, Bartz J. 1997. The control of strawberry diseases by sanitation. *Acta Hort.* 439:917–922.
- Legard D, MacKenzie S, Mertely J, Chandler C, Peres N. 2005. Development of a reduced use fungicide program for control of *Botrytis* fruit rot on annual winter strawberry. *Plant Dis.* 89: 1353–1358.
- Lenth RV. 2021. emmeans: Estimated Marginal Means, aka Least-Squares Means. R Package Version 1.5.5-1.
- Lerceteau-Köhler E, Moing A, Guérin G, Renaud C, Petit A, et al. 2012. Genetic dissection of fruit quality traits in the octoploid cultivated strawberry highlights the role of homoeo-qtL in their control. *Theor Appl Genet.* 124:1059–1077.
- Leroux P. 2007. Chemical control of *Botrytis* and its resistance to chemical fungicides. In: *Botrytis: Biology, Pathology and Control*. Springer. p. 195–222.
- Lewers KS, Luo Y, Vinyard BT. 2012. Evaluating strawberry breeding selections for postharvest fruit decay. *Euphytica.* 186: 539–555.
- Lin Z, Hayes B, Daetwyler H. 2014. Genomic selection in crops, trees and forages: a review. *Crop Pasture Sci.* 65:1177–1191.
- Lorang J. 2019. Necrotrophic exploitation and subversion of plant defense: a lifestyle or just a phase, and implications in breeding resistance. *Phytopathology.* 109:332–346.
- Lurie S, Fallik E, Handros A, Shapira R. 1997. The possible involvement of peroxidase in resistance to *Botrytis cinerea* in heat treated tomato fruit. *Physiol Mol Plant Pathol.* 50:141–149.
- Margarido GR, Souza AP, Garcia AA. 2007. OneMap: software for genetic mapping in outcrossing species. *Hereditas.* 144:78–79.
- Meyer D, Dimitriadou E, Hornik K, Weingessel A, Leisch F. 2019. E1071: Misc Functions of the Department of Statistics, Probability Theory Group (Formerly: E1071), TU Wien. R Package Version 1.7-4. <https://CRAN.R-project.org/package=e1071>.
- Mitcham B, Cantwell M, Kader A. 1996. Methods for determining quality of fresh commodities. *Perishables Handl Newslett.* 85:1–5.
- Moriya Y, Itoh M, Okuda S, Yoshizawa AC, Kanehisa M. 2007. KAAS: an automatic genome annotation and pathway reconstruction server. *Nucleic Acids Res.* 35:W182–W185.
- Pérez P, de Los Campos G. 2014. Genome-wide regression and prediction with the BGLR statistical package. *Genetics.* 198:483–495.
- Petrasch S, Knapp SJ, Van Kan JA, Blanco-Ulate B. 2019a. Grey mould of strawberry, a devastating disease caused by the ubiquitous necrotrophic fungal pathogen *Botrytis cinerea*. *Mol Plant Pathol.* 20:877–892.
- Petrasch S, Silva CJ, Mesquida-Pesci SD, Gallegos K, van den Abeele C, et al. 2019b. Infection strategies deployed by *Botrytis cinerea*, *Fusarium acuminatum*, and *Rhizopus stolonifer* as a function of tomato fruit ripening stage. *Front Plant Sci.* 10:223.
- Poland J, Rutkoski J. 2016. Advances and challenges in genomic selection for disease resistance. *Annu Rev Phytopathol.* 54: 79–98.
- Quidde T, Osbourn A, Tudzynski P. 1998. Detoxification of α -tomatine by *Botrytis cinerea*. *Physiol Mol Plant Pathol.* 52:151–165.
- R Core Team. 2021. R: A Language and Environment for Statistical Computing. R Foundation for Statistical Computing. Vienna, Austria.
- Rhainds M, Kovach J, English-Loeb G. 2002. Impact of strawberry cultivar and incidence of pests on yield and profitability of strawberries under conventional and organic management systems. *Biol Agric Hortic.* 19:333–353.
- Ries SM. 1995. Gray mold of strawberry. University of Illinois Integrated Pest Management Program Reports on Plant Diseases 704. <http://ipm.illinois.edu/diseases/series700/rpd704/>.
- Rowe HC, Kliebenstein DJ. 2008. Complex genetics control natural variation in *Arabidopsis thaliana* resistance to *Botrytis cinerea*. *Genetics.* 180:2237–2250.
- Rueden CT, Schindelin J, Hiner MC, DeZonia BE, Walter AE, et al. 2017. ImageJ2: imageJ for the next generation of scientific image data. *BMC Bioinform.* 18:529.
- Rutkoski JE, Heffner EL, Sorrells ME. 2011. Genomic selection for durable stem rust resistance in wheat. *Euphytica.* 179: 161–173.
- Rutkoski JE, Poland JA, Singh RP, Huerta-Espino J, Bhavani S, et al. 2014. Genomic selection for quantitative adult plant stem rust resistance in wheat. *Plant Genome.* 7:1–10. doi:10.3835/plantgenome2014.02.0006.
- Saijo Y, Loo E. P-I, Yasuda S. 2018. Pattern recognition receptors and signaling in plant-microbe interactions. *Plant J.* 93:592–613.
- Schiffthaler B, Bernhardsson C, Ingvarsson PK, Street NR. 2017. BatchMap: a parallel implementation of the OneMap R package for fast computation of F1 linkage maps in outcrossing species. *PLoS One.* 12:e0189256.
- Schindelin J, Arganda-Carreras I, Frise E, Kaynig V, Longair M, et al. 2012. Fiji: an open-source platform for biological-image analysis. *Nat Methods.* 9:676–682.
- Seijo TE, Chandler CK, Mertely JC, Moyer C, Peres NA. 2008. Resistance of strawberry cultivars and advanced selections to anthracnose and *Botrytis* fruit rots. *Proc Florida State Hort Soc.* 121:246–248.
- Silva CJ, van den Abeele C, Ortega-Salazar I, Papin V, Adaskaveg JA, et al. 2021. Host susceptibility factors render ripe tomato fruit vulnerable to fungal disease despite active immune responses. *J Exp Bot.* 72:2696–2709.
- Tomas-Grau RH, Requena-Serra FJ, Hael-Conrad V, Martínez-Zamora MG, Guerrero-Molina MF, et al. 2018. Soft mechanical stimulation induces a defense response against *Botrytis cinerea* in strawberry. *Plant Cell Rep.* 37:239–250.
- van Baarlen P, Legendre L, van Kan JA. 2007. Plant defence compounds against *Botrytis* infection. In: *Botrytis: Biology, Pathology and Control*. Springer. p. 143–161.
- van Kan JA. 2006. Licensed to kill: the lifestyle of a necrotrophic plant pathogen. *Trends Plant Sci.* 11:247–253.
- Van Os H, Stam P, Visser RG, Van Eck HJ. 2005. RECORD: a novel method for ordering loci on a genetic linkage map. *Theor Appl Genet.* 112:30–40.
- van Schie CC, Takken FL. 2014. Susceptibility genes 101: how to be a good host. *Annu Rev Phytopathol.* 52:551–581.
- VanRaden P. 2020. Symposium review: how to implement genomic selection. *J Dairy Sci.* 103:5291–5301.
- Veloso J, van Kan JA. 2018. Many shades of grey in *Botrytis* – host plant interactions. *Trends Plant Sci.* 23:613–622.
- Verma S, Zurn JD, Salinas N, Mathey MM, Denoyes B, et al. 2017. Clarifying sub-genomic positions of qtls for flowering habit and fruit quality in us strawberry (*Fragaria × ananassa*) breeding populations using pedigree-based qtl analysis. *Hortic Res.* 4:9.
- Voss-Fels KP, Cooper M, Hayes BJ. 2019. Accelerating crop genetic gains with genomic selection. *Theor Appl Genet.* 132:669–686.
- Williamson B, Tudzynski B, Tudzynski P, Van Kan JA. 2007. *Botrytis cinerea*: the cause of grey mould disease. *Mol Plant Pathol.* 8: 561–580.
- Zhang W, Corwin JA, Copeland DH, Feusier J, Eshbaugh R, et al. 2019. Plant-necrotroph co-transcriptome networks illuminate a metabolic battlefield. *eLife.* 8:e44279.
- Zhang Y, Butelli E, De Stefano R, Schoonbeek H-J, Magusin A, et al. 2013. Anthocyanins double the shelf life of tomatoes by delaying

- overripening and reducing susceptibility to gray mold. *Curr Biol.* 23:1094–1100.
- Zheng Y, Jiao C, Sun H, Rosli HG, Pombo MA, et al. 2016. iTAK: a program for genome-wide prediction and classification of plant transcription factors, transcriptional regulators, and protein kinases. *Mol Plant.* 9:1667–1670.
- Zorrilla-Fontanesi Y, Cabeza A, Domínguez P, Medina JJ, Valpuesta V, et al. 2011. Quantitative trait loci and underlying candidate genes controlling agronomical and fruit quality traits in octoploid strawberry (*Fragaria × ananassa*). *Theor Appl Genet.* 123:755–778.

Communicating editor: J.-L. Jannink